Mapping Cluster Magnetic Fields Using Faraday Rotation Measures

G. B. Taylor[1], S. W. Allen[2] and A. C. Fabian[2]

[1] National Radio Astronomy Observatory, Soccoro, NM 87801, U.S.A.
[2] Institute of Astronomy, Madingley Road, Cambridge CB3 OHA, U.K.

Abstract. We present an update on work in progress to understand the origin high Faraday Rotation Measures in extragalactic radio sources. One established mechanism of producing high RMs is magnetized cluster gas. New observations of the radio galaxy PKS 1246−410 in the Centaurus cluster are presented here, and observations of a sample of 14 cooling flow clusters with embedded radio galaxies are summarized. A correlation is apparent between the cooling flow rate and the maximum Faraday Rotation Measures. Magnetic fields of strength 10–100 μG are found to be common to most clusters.

1. Introduction

Radio sources embedded within rich clusters of galaxies can serve as useful probes of the intracluster medium (ICM). Sharp changes in the ICM pressure at the sonic radius may disrupt radio jets (Soker & Sarazin 1988; Norman, Burns & Sulkanen 1988), and if the thermal ICM pressure is large enough it may confine the radio source. Polarized radiation from embedded radio sources may also be rotated by the Faraday effect if magnetic fields are present in the ICM.

The X-ray emission in some clusters is strongly peaked at the center, leading to high densities and cooling times of the hot ICM in the inner ~100 kpc of much less than the Hubble time. To maintain hydrostatic equilibrium, an inward flow is required (for a review see Fabian, Nulsen & Canizares 1991; see also contributions by Fabian and by Allen within these proceedings). Typical mass cooling flow rates are 100 $\mathrm{M}_\odot\ \mathrm{yr}^{-1}$. The cooling flow phenomenon in clusters is quite common - between 70-90% of an X-ray flux-limited sample of clusters have cooling flows (Edge, Stewart & Fabian 1992).

While most extragalactic radio sources exhibit Faraday rotation measures (RMs) on the order of 10s of rad m^{-2} due to the interstellar medium of our galaxy, there are a small number of sources displaying RMs in excess of ~1000 rad m^{-2}. Studies of these high RM sources (e.g. Cygnus A: Dreher, Carilli & Perley 1987; A1795: Ge & Owen 1993; Hydra A: Taylor & Perley 1993) indicate that these RMs are most likely to be induced by a cluster magnetic field. Furthermore a common theme has emerged that each of the high RM sources is found in association with a hot X-ray emitting gas, and in most cases a cooling flow (Taylor, Barton & Ge 1994). The diversity of the radio structures and powers, and the commonality of the X-ray parameters suggest that the high RMs are the result of external Faraday rotation occurring in a magnetized hot cluster gas surrounding the radio sources. For external Faraday rotation, the RMs are related to the density, n_e, and magnetic field along the line-of-sight, $B_\|$, through the cluster according to

$$RM = 812 \int_0^L n_\mathrm{e} B_\| \mathrm{d}l \text{ radians m}^{-2} , \qquad (1)$$

where $B_\|$ is measured in μGauss, n_e in cm^{-3} and dl in kpc. The RM distribution, along with X-ray observations (used to estimate n_e), can then be used to understand the magnetic field structure along the line-of-sight.

The RM structure of many of the high RM sources (in particular that of Hydra A, 3C 295, Cygnus A, and A1795) show ordered structures over tens to hundreds of kpc. The origin and evolution of such magnetic fields is a topic of some speculation (Daly & Loeb 1990; Goldman & Rephaeli 1991; DeYoung 1992). They could be remnant magnetic fields of extinct radio galaxies, the result of a cluster dynamo effect (Ruzmaikan et al.1989), or magnetic fields stripped from spiral galaxies during galactic cannibalism. Cluster magnetic fields may have important effects on cluster dynamics and energy transport (Sarazin 1986; and see contribution by Chandran in these proceedings), and significant implications for primordial star formation (Pudritz & Silk 1990). These magnetic fields can only be traced when there is a radio source located within or behind the cluster. Clarke and collaborators (these proceedings) discuss the use of sources fortuitously located behind clusters and strong enough to provide a good estimate of the RM. Unfortunately, the number of such sources are not large, and obtaining the RMs requires a considerable amount of observing time. Here, we discuss the use of clus-

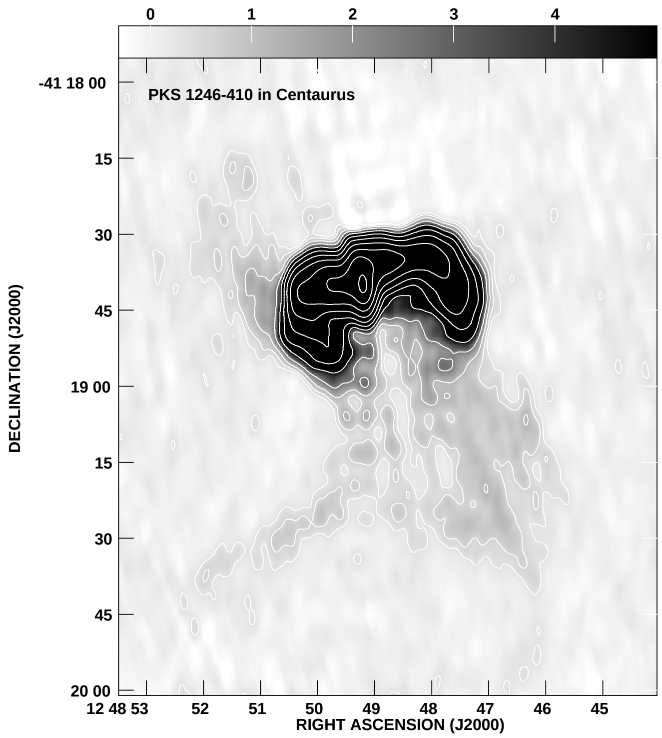

Fig. 1. VLA image of PKS 1246-410 at 1.565 GHz. The greyscale has been chosen to show the faint extended emission in the range 0 to 5 mJy/beam. Contours start at 0.3 mJy/beam and increase by factors of 2. The peak flux density in the map is 358 mJy/beam. The restoring beam has dimensions 4.4 × 2.1 arcsec in position angle 0 degrees.

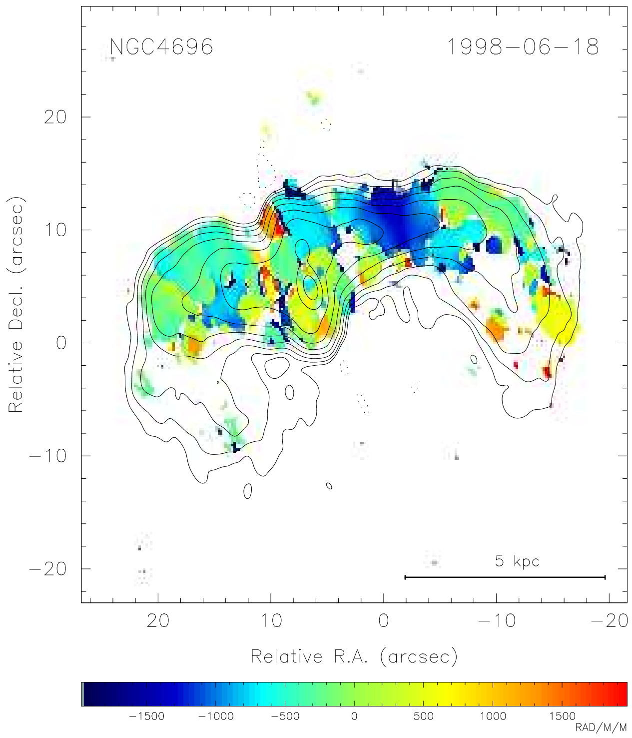

Fig. 2. The rotation measure (RM) map for PKS 1246-410 at the center of the Centaurus cluster. Contours are taken from the 4.8 GHz total intensity image.

ters with known embedded radio sources. We assume $H_0 = 50$ km s^{-1} Mpc^{-1} and $\Omega = 1$ throughout.

2. RMs in the Centaurus Cluster

At this point the somewhat checkered history of this project can serve to illustrate the benefits of bringing X-ray and radio astronomers together as was done so well by the organizers of this conference. The Edge et al. sample listed substantial cooling flows in the Centaurus and the 3C 129 cluster, but did not provide any coordinates. Going on the name alone, Taylor, Barton & Ge (1994) mistook Centaurus A and 3C 129 as the radio sources of interest in those clusters. It has taken a number of years and some face-to-face meetings with X-ray astronomers to discover that the radio sources embedded in the Centaurus and 3C 129 cooling flows are PKS 1246-410 and 3C 129.1 respectively. Here we present some long awaited VLA[1] observations results on the heretofore little known radio galaxy PKS 1246-410 in the Centaurus cluster.

The radio source PKS 1246-410 is associated with NGC 4696, an elliptical galaxy at the center of the Centaurus cluster (also known as Abell 3526). The redshift is 0.0099, so 1 arcsecond corresponds to 0.28 kpc. The radio power of PKS 1246-410 is 1.5 $\times 10^{24}$ W Hz^{-1} at 1.6 GHz, placing it firmly as a low power radio galaxy for which we would expect an FR 1 morphology (edge dimmed "woofly" radio tails). In fact the radio morphology at 1.6 GHz (see Fig. 1), appears quite different from most low power radio galaxies. The usual well defined core and thin jets feeding into larger lobes are missing. Instead there is a bright point source which we identify as the core based on its central location and slightly flatter spectral index of $\alpha = -0.5$, where $S_\nu \propto \nu^\alpha$. The core is surrounded by "lobe" emission with a predominantly east-west orientation. At their extremes both lobes appear (at least in projection) bent to the south and back in towards

[1] The National Radio Astronomy Observatory is a facility of the National Science Foundation operated under a cooperative agreement by Associated Universities, Inc.

Table 1. Radio Sources in Cooling Flow Clusters

Cluster	Radio Source	z	$\dot{M}^a$ ($M_\odot\ yr^{-1}$)	$\dot{M}^b$ ($M_\odot\ yr^{-1}$)	log L_x (erg s^{-1})	Gal.[c] Type	S_{5000} (Jy)	log P_{5000} (W Hz^{-1})	Size[d] (kpc)	$RM(1+z)^2$ (rad m^{-2})	Ref.
Cygnus A	3C 405	0.057	187	320^{+71}_{-32}	44.8	E	364	27.7	180	3000	1
Virgo	3C 274	18 Mpc	10	$24^{+10.6}_{-5.7}$	43.1	E	76	24.4	58	2000	2
A426	3C 84	0.0183	183	587^{+86}_{-44}	45.0	*pec*	50	25.9	640	N/A	4
Hydra A	3C 218	0.0522	315	267^{+48}_{-30}	44.5	cD	14	26.3	670	−12000	5
Centaurus	1246−410	0.0099	18	$39^{+25.5}_{-7.8}$	43.8	E	1.4	25.8	15	1500	3
A2052	3C 317	0.0348	90	125^{+26}_{-6}	44.1	cD	1.0	24.7	39	−800	6
A2199	3C 338	0.031	150	197^{+20}_{-41}	44.5	cD	0.48	24.3	67	2000	6
A119	0053−015	0.044	23	0^{+2}_{-0}	44.4	E	0.40	24.5	350	400	7
	0053−016	0.044	23	0^{+2}_{-0}	44.4	E	0.29	24.4	300	150	7
0745−191	0745−191	0.1028	702	1038^{+116}_{-68}	45.4	cD	0.39	25.3	25	N/A	8
A2597	2322−123	0.0824	480	423^{+91}_{-99}	44.8	cD	0.33	25.0	10	4700	9
A1795	4C 26.42	0.062	478	462^{+108}_{-56}	44.9	cD	0.26	24.6	15	3000	6
3C 129	0445+449	0.0208	61	$0^{+4.2}_{-0}$	44.3	E	0.25	23.7	500	300	9
A4059	2354−350	0.0478	124	115^{+57}_{-37}	44.3	cD	0.11	24.0	70	−1500	8
A2029	1508+059	0.0767	402	590^{+27}_{-96}	45.3	cD	0.10	24.4	80	−8000	8

[a] The mass flow rate for a critical cooling time of 2×10^{10} from Edge, Stewart & Fabian (1992).
[b] Recent x-ray measurements of mass flow rate for a critical cooling time of 1.3×10^{10} yr from Allen et al. in prep, Allen & Fabian (1997), Peres et al.(1998), and White, Jones & Forman (1997).
[c] Galaxy type (E:elliptical; pec: peculiar, or cD: central dominant elliptical)
[d] The largest angular size of the radio source in kpc.
References - (1) Dreher et al. 1987; (2) Owen et al. 1990; (3) Taylor, Allen & Fabian, in prep; (4) Burns et al. 1992; (5) Taylor & Perley 1993; (6) Ge & Owen 1993; (7) Feretti et al.1999; (8) Taylor, Barton, & Ge 1994; (9) Taylor, in prep.

the core, although there is also a weak extension to the northeast. The emission in the extremities is quite steep ($\alpha \sim -2$). Overall the impression is of a rather distorted radio morphology, perhaps due to confinement by the hot X-ray emitting gas. Similar morphologies have been seen for other radio galaxies embedded in dense X-ray environments with the most extreme case being the amorphous radio galaxy PKS 0745-191 (Taylor, Barton & Ge 1994).

Fortunately the bright radio lobes of PKS 1246-410 are moderately well polarized (5 – 40%), so it is possible to derive the RM distribution across nearly the entire radio source. This has been done using four frequencies spread across the 4 and 6 cm bands, and is shown in Figure 2. The RMs appear patchy and are not correlated with any features in total intensity. The RMs in PKS 1246-410 are typically in the range −500 to +500 rad m^{-2} and reach a maximum of 1500 rad m^{-2}.

The gas density profile derived from ROSAT HRI observations can be parameterized as a simple power-law, $n(r) = n_0 r^{-\alpha}$ with a slope $\alpha = 0.93$ and an electron density at radius 10 kpc of 0.039 cm^{-3}. Considering the patch of −1500 rad m^{-2} located 3 kpc west of the core, the minimum constant magnetic field, $B_\parallel$, that could produce the observed RM has a strength of 17 μG. Several changes in sign are in evidence on both sides of the core, however, indicating that the magnetic field direction is rather chaotic. The simplest explanation for the RM distribution is a tangled magnetic field with a coherence length of ~1 kpc. To first order the magnetic field required will be larger by $\sqrt{N}$ where N is the number of cells. For Centaurus this results in a revised estimate for $B_\parallel$ of 90 μG. More realistic models in which the magnetic field strength also follows a power law distribution are being considered.

3. A sample of radio sources embedded in cooling flow clusters

Examination of a flux-limited, all-sky X-ray sample of galaxies put forth by Edge, Stewart, & Fabian (1992) reveals that clusters with non-zero mass flow rates frequently display significant RMs. Taylor, Barton & Ge (1994) formed a sample of 14 cooling flow clusters each containing at least one embedded radio galaxy stronger than 100 mJy at 5 GHz. Here we present a refinement and progress report for that sample.

Of the 14 clusters in the sample, 10 display an excess of 800 rad m^{-2}, two have RMs between 300 and 700 rad m^{-2} (one is A119 discussed by Feretti et al. 1999 and by Govoni et al. in these proceedings; and one of these is the 3C 129 cluster in which the RMs at the cluster center towards 3C 129.1 have not yet been measured), and two could not be measured (PKS0745-191 and A426) due to a lack of polarized flux. Cooling flow rates, X-ray luminosi-

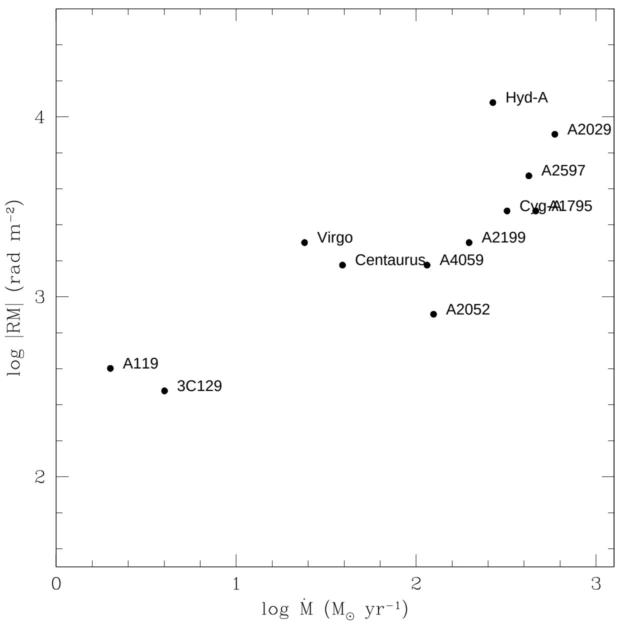

Fig. 3. The maximum absolute RM plotted as a function of $\dot{M}$ for the 12 clusters in Table 5 with measured RMs. Note that the RMs in the 3C 129 cluster have not yet been measured toward 3C 129.1 in the cluster center, so the maximum RM is likely to be considerably greater.

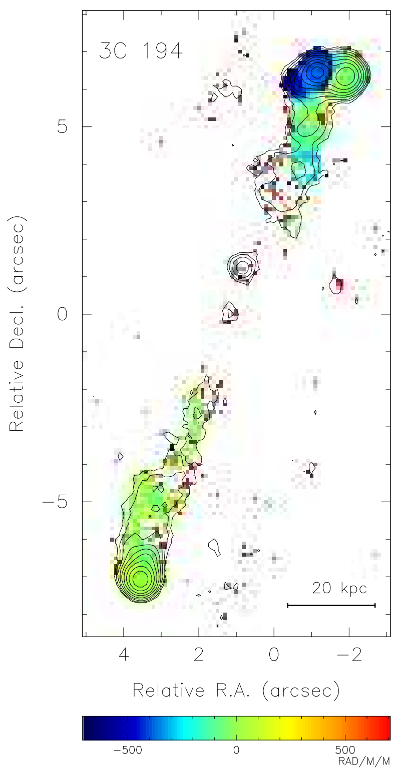

Fig. 4. The RM structure of 3C 194 at 0.4 arcsec resolution. The colorbar runs from -700 to $+700$ rad m^{-2}. The RM values in the rest frame of the source are larger by a factor of 4.8. Contours from the 6 cm total intensity image are overlaid.

ties (from 2-10 keV), RMs, and other relevant parameters for these 14 clusters are listed in Table 1. The RM value given is chosen from the region of largest RM which is coherent across a beamwidth or more with good polarized signal-to-noise. We have also plotted in Fig. 3 the RM as a function of cooling rate, $\dot{M}$. These results strongly suggest a correlation between the cooling rate and rotation measure. Even more striking is the fact that *all* of the known high RM sources (RM $>$ 700 rad m^{-2}; see Table 1 in Taylor, Inoue, & Tabara 1992b) at low redshifts ($z < 0.4$) are included in this X-ray selected sample. The high RM radio galaxy 3C 295 (Perley & Taylor 1991) at a redshift of 0.461 is also associated with a luminous X-ray cooling flow (Henry & Henriksen 1986), but the X-ray data for the remaining seven high RM, high z, sources are not good enough to distinguish between extended thermal emission and that from an active nuclear source. Beyond redshifts of ∼0.4, low power radio sources like PKS 1508+059, and PKS 2354−350 are much too weak to allow for a determination of their RM.

4. Extrapolating to high redshift

Most of the high RM sources found at redshifts greater than 0.4 are CSS (compact steep spectrum) sources which have large radio powers and small sizes. Another mechanism to produce high RMs, however, has recently come to light. Udomprasert et al. (1997) found that the high RMs in the CSS quasar OQ 172 were entirely associated with the nuclear component. So it is likely that the high RMs in some, or even all, CSS sources do not have a cluster origin. In fact, Taylor (1998) has demonstrated that the cores of most quasars exhibit high RMs when observed with sufficiently high angular resolution.

With the above caveat in mind, it may still be worthwhile to speculate that the high RMs seen towards some larger, extended radio galaxies may originate in a cluster magnetic field. Taylor, Inoue, & Tabara (1992a) measured high RMs in the radio galaxy 3C 194 at z=1.185, and suggest that these could be the result of a cluster magnetic field. Carilli et al. (1997) found high RMs in 6/37 radio galaxies beyond z=2. ROSAT observations of one of these, 1138−262, has revealed a marginally extended source that at z=2.156 could be the highest redshift cluster yet discovered (Carilli et al. 1998). The existence of clustering at high redshift has important ramifications for cosmological models.

The RM distribution for 3C 194 is reproduced in Figure 4. It is worth noting that 3C 194 has an unusual RM distribution, in that the RMs are small across most of the source, and are high only at the location of the northern hot spot. The RM distribution in 1138–262 is similar with the region of high RM confined to a single hot spot. A possible explanation for this effect is that the external gas and magnetic fields are enhanced by the bowshock associated with the hot spot.

5. Conclusions

Cluster magnetic fields can explain many, but not all, of the high rotation measure (RM > 1000 rad m^{-2}) sources. Observations of the Faraday rotation measure distribution of radio sources embedded in clusters can provide unique information about the coherence length of the fields, and combined with estimates of the thermal gas density from X-ray observations, yield estimates of the magnetic field strength. The discovery of high RMs in extended high-redshift radio galaxies may serve as a signpost indicating dense cluster gas in the early universe.

Acknowledgements. This research has made use of the NASA/IPAC Extragalactic Database (NED) which is operated by the Jet Propulsion Laboratory, Caltech, under contract with NASA.

References

Allen, S.W., & Fabian, A.C. 1997, MNRAS 286, 583
Burns, J.O., Sulkanen, M.E., Gisler, G.R., & Perley, R.A. 1992, ApJ 388, L49
Carilli, C.L., Rottgering, H.J.A., van Ojik, R., Miley, G.K., & van Breugel, W.J.M. 1997, ApJS 109, 1
Carilli, C.L., Harris, D.E., Pentericci, L., Rottgering, H.J.A., Miley, G.K., & Bremer, M.N. 1998, ApJ 494, L143
Daly, R.A., & Loeb, A. 1990, ApJ 364, 451
DeYoung, D.S. 1992, ApJ 386, 464
Dreher, J.W., Carilli, C.L., & Perley, R.A. 1987, ApJ 316, 611
Edge, A.C., Stewart, G.C., & Fabian, A.C. 1992, MNRAS 258, 177
Fabian, A.C., Nulsen, P.E.J., & Canizares, C.R. 1991, A&A Rev., 2, 191
Feretti, L., Dallacasa, D., Govoni, F., Giovannini, G., Taylor, G.B., & Klein, U. 1999, A&A 344, 472
Ge, J.P., & Owen F.N. 1993, AJ 105, 778
Goldman, I., & Rephaeli, Y., 1991, ApJ 380, 344
Henry, J.P., & Henriksen, M.J. 1986, ApJ 301, 689
Norman, M.L., Burns, J.O., & Sulkanen, M.E. 1988, Nature 355, 146
Owen, F.N., Eilek, J.A., & Keel, W.C. 1990, ApJ 362, 449
Peres, C.B., Fabian, A.C., Edge, A.C., Allen, S.W., Johnstone, R.M., & White, D.A. 1998, MNRAS 298, 416
Perley, R.A., & Taylor, G.B. 1991, AJ 101, 1623
Pudritz, R.E., & Silk, J. 1989, ApJ 342, 650
Ruzmaikan, A.A., Sokoloff, D.D., & Shukurov, A. 1989, MNRAS 241, 1
Sarazin, C.L. 1986, Rev. Mod. Phys. 58, 1.
Soker, N., & Sarazin, C.L. 1988, ApJ 327, 66
Taylor, G.B., Inoue, M., & Tabara, H. 1992a, A&A, 264, 415
Taylor, G.B., Inoue, M., & Tabara, H. 1992b, A&A, 264, 421
Taylor, G.B., & Perley, R.A. 1993, ApJ 416, 554
Taylor, G.B., Barton, E.J., & Ge, J.-P. 1994, AJ 107, 1942
Taylor, G.B. 1998, ApJ 506, 637
Udomprasert, P.S., Taylor, G.B., Pearson, T.J., & Roberts, D.H. 1997, ApJ 483, L9-L12
White, D.A., Jones, C., & Forman, W. 1997, MNRAS 292, 419